Technical University of Denmark

DTU

An adaptive, data driven sound field control strategy for outdoor concerts

Heuchel, Franz Maria; Caviedes Nozal, Diego; Brunskog, Jonas; Fernandez Grande, Efren; Agerkvist, Finn T.

Published in:
Proceedings of 2017 AES International Conference on Sound Reinforcement

Publication date:
2017

Document Version
Peer reviewed version

Link back to DTU Orbit

DTU Library
Technical Information Center of Denmark

An adaptive, data driven sound field control strategy for outdoor concerts

Franz M. Heuchel[1], Diego Caviedes Nozal[1], Jonas Brunskog[1], Efren Fernandez Grande[1], and Finn T. Agerkvist[1]

[1]*Technical University of Denmark, Department of Electrical Engineering, Acoustic Technology Group*

Correspondence should be addressed to Diego Caviedes Nozal and Franz Heuchel (`dicano@elektro.dtu.dk`, `fmheu@elektro.dtu.dk`)

ABSTRACT

One challenge of outdoor concerts close to urban environments is to ensure adequate levels for the audience while avoiding disturbance of the surrounding residential areas. This paper outlines the initial concept of a sound field control system for tackling this issue. The idea is to create acoustic contrast between the audience area and the surrounding using methods from sound zoning. Control over large areas implies the need for precise information of transfer-functions between the loudspeakers and the control areas. The envisioned system uses a combination of measurements and Bayesian inference to update the parameters of a sound propagation model which estimates these transfer-functions. We present a simple case in which sound field control and propagation model work together.

1 Introduction

Outdoor music events in urban environments face the challenge to both deliver an excellent concert experience and comply with the local regulations on sound exposure of neighboring residential areas. If the regulations limit the achievable sound pressure levels (SPL) inside the audience area too much, the audio experience can degrade severely as high SPL is an essential part of the concert experience. At the same time, these regulations are important as exposure to excessive noise levels is known to have a negative impact on quality of life.

Active sound field control methods based on sound zones principles have been shown to produce significant SPL differences (acoustic contrast) between control areas, using methods from sound zoning [1, 2, 3] or beamforming [4, 5]. The *first hypothesis* of this work is that such sound field control methods can be applied in large-scale outdoor concerts to focus and contain the low frequency sound more efficiently on the audience area. We believe that this could substantially enhance the trade-off between SPL in the audience area and sound exposure of neighboring residents.

Most modern sound reinforcement systems are based on the line array principle, which allows for the control of directivity of the sound radiation of high and mid frequencies. However, the radiation of low frequencies, can not be as easily controlled, they are less attenuated by air and reflections from boundaries, and are damped the least by the structures of residential buildings. Low frequencies are therefore the most critical frequencies in the noise problem of outdoor concerts. As controlling the sound field over large areas with a feasible number of loudspeakers is restricted to low frequencies, we believe that such a technology is a good fit for this problem.

Accurate estimations of the transfer-function between the loudspeakers and the control regions is essential for the optimization of loudspeaker filters. The two approaches for estimation of transfer-functions are direct measurement and prediction using numerical methods. In large scale outdoor applications, the former is infeasible, because the sound field has to be sampled with respect to the Nyquist theorem to avoid aliasing problems, leading to a large amount of measurement points. The latter is too inaccurate for control purposes due to uncertainties in the model parameters, e.g. the reflection coefficients of boundaries or the atmospheric conditions. It is our *second hypothesis* that the accuracy of the sound propagation model can be improved by simultaneously measuring two sources of real-time data: 1) Weather conditions (wind, humidity and temperature) to construct the prediction model and 2) a small set of pressure transfer-functions over the control areas to correct and update the acoustic parameters and validate the model. The parameter estimation is done by applying the Bayesian inference framework,

which has been shown to work well in similar regression problems [6, 7, 8]. Bayesian inference is adequate for working with constrained multiparameter models including noise and uncertainty effects.

In the current work we present our first ideas for such a sound field control system for outdoor concerts, illustrate the basic concepts using a simple simulation, and discuss the challenges of a real implementation of such a technology.

The paper is structured as follows. Section 2 gives an overview of the closed loop architecture of the sound field control system. Section 3 describes the methods used for the sound zoning, Bayesian inference and the propagation model. In section 4, the methods are applied to a simple simulation example. Section 5 and section 6 discuss the simulation results and highlight some of the challenges of controling sound fields for outdoor concerts.

2 Concept

The fundamental concept of the sound field control system is shown in figure 1. There are two main functional modules: the sound field controller and the sound propagation model. In an initialization phase, the propagation model is fed with the constant model parameters like loudspeaker positions, directivities, venue geometries, acoustic parameters of the occurring surfaces, and pre-measured transfer-functions between the sources and the regions in which the sound is to be controlled. An initial estimate of the transfer-functions is then calculated and fed to the sound field controller. The sound field controller derives the optimal loudspeaker filters using the estimated transfer-functions from the propagation model. Internet-of-Things (IoT) enabled sensors distributed throughout the venue and its surroundings are connected to a dedicated cloud and gather real-time sound pressure and meteorological data. The propagation model uses this information to continuously update its model parameters and the estimate of the transfer-functions. The information can then also be shared with the IoT cloud, e.g. a noise map of the venue and it's surroundings can be provided to the event organizers or sound engineers.

This system is planned to be part of the EU project MONICA [9], whose goal is the integration of IoT technologies and enabled IoT devices into a common platform to improve the experience of citizens in large outdoor events.
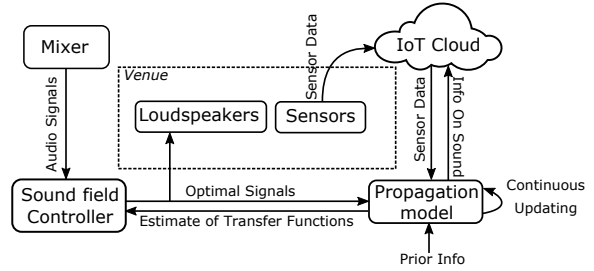

Fig. 1: Information flow in the sound field control system.

3 Methods

3.1 Sound Field Optimization

Sound field optimization is the sound field controller's main function. The term describes methods that create a desired target sound field by optimization of each loudspeakers input signal. These are applied for instance in the creation of sound zones, i.e. spatially extended zones with different acoustic characteristics. In this work we want to create two sound zones: a bright zone in the audience area with a homogeneous sound field in space and frequency and a dark zone in the surrounding neighborhood in which the sound pressure is as low as possible. The loudspeaker filters that create such a sound field can be derived from the solution of an optimization problem. Here we use the combination of pressure-matching and acoustic contrast control proposed by Chang and Jacobsen [1] and formulated by Betlehem et al. [3] as a constraint optimization problem, which minimizes the reproduction error in the bright zone while restricting the mean square pressure in the dark zone.

The sound pressure field p in the bright zone (BZ) and the dark zone (DZ) is sampled spatially at J_{BZ} evaluation points $\mathbf{r}_j, j \in$ BZ, at J_{DZ} evaluation point positions $\mathbf{r}_j, j \in$ DZ and at N frequencies $f^{(n)}$ with frequency resolution Δf. It can then be represented by coefficients $p_j^{(n)}$. Let there be loudspeakers positioned outside the two zones at I positions $\mathbf{s}_i$. The total sound pressure at each frequency n and evaluation point j is

$$p_j^{(n)} = \sum_{i=1}^{I} H_{ij}^{(n)} q_i^{(n)}, \qquad (1)$$

where $H_{ij}^{(n)}$ denotes the transfer-function between sources and evaluation points at the given frequency

and $q_i^{(n)}$ denotes the complex weight or filter coefficients for each source and frequency.

The goal of the optimization is to find the optimal set of loudspeaker weights which minimize the relative mean square error in the bright zone between the target field $p_j^{\text{t},(n)}$ and the realized field $p_j^{(n)}$, while constraining both the mean square pressure in the dark zone and the frequency-integrated mean square of the loudspeaker strengths, i.e.

$$\min_{\mathbf{q}} \quad \frac{1}{J_{\text{BZ}}N} \sum_{i\in\text{BZ}} \sum_{n=1}^{N} \frac{|p_j^{\text{t},(n)} - p_j^{(n)}|^2}{|p_j^{\text{t},(n)}|^2}$$

$$\text{s. t.} \quad \frac{1}{J_{\text{DZ}}} \sum_{i\in\text{DZ}} |p_j^{(n)}|^2 \le D_0 \quad \forall n = 1,\ldots,N. \quad (2)$$

$$\frac{1}{I} \sum_{i=0}^{I} \sum_{n=1}^{N} |q_i^{(n)}|^2 \Delta f \le E_0$$

This is an inverse problem and the constraint on the square of the source strengths acts as a regularization. The quadratically constrained quadratic problem is convex, if the transfer-functions are such that for each frequency $\mathbf{H}^{(n)H}\mathbf{H}^{(n)}$ is semi-definite, where $[\mathbf{H}^{(n)}]_{ij} = H_{ij}^{(n)}$ [10].

The problem is solved using the Sequential Linear Squares Programming algorithm of SciPy's optimization module [11].

3.2 Propagation model

One of the most common outdoor sound propagation models in Nordic countries is Nord2000 [12], which is based on the image source method. A simplified version is used in this paper to show how Bayesian inference could improve its performance.

In this simplified model, the loudspeakers are assumed monopole sources with a constant frequency response. The total pressure at each evaluation point is the sum of the pressure generated by each source and its reflections from the ground. The transfer-function for each source-evaluation point combination and frequency is

$$H_{ij}^{(n)} = \frac{\text{j}\rho}{4\pi} \left(\frac{e^{-\text{j}\frac{2\pi f^{(n)}}{c}r_{ij}^{\text{d}}}}{r_{ij}^{\text{d}}} + R\frac{e^{-\text{j}\frac{2\pi f^{(n)}}{c}r_{ij}^{\text{i}}}}{r_{ij}^{\text{i}}} \right), \quad (3)$$

where r_{ij}^{d} and r_{ij}^{i} are the direct and indirect path lengths between sources and evaluation points. For the sake of simplicity, ground reflections at an angle α are modelled with a plane wave reflection coefficient $R = \frac{Z\cos(\alpha)+\rho c}{Z\cos(\alpha)-\rho c}$ and the Miki model for the ground impedance [13]

$$Z = \rho c \left(1 + 5.51\left(\frac{1000f}{\sigma}\right)^{-0.632} \right. \quad (4)$$

$$\left. - j8.42\left(\frac{1000f}{\sigma}\right)^{-0.632} \right).$$

Even though the spherical reflection coefficient is a much more precise model of the reflection, it will not affect the purpose of this paper.

3.3 Bayesian Inference and Parameter Estimation

Moving from simulated scenarios to real measurements implies that most of the parameters involved are only known with some uncertainty, causing wrong propagation predictions. Bayesian inference is a method to find better estimates of these parameters on the basis of data. In this section the present problem is formulated in terms of Bayes' theorem and an example of normal non-linear regression is presented.

Bayes' theorem [14] states that given a set of measured pressure data $\tilde{\mathbf{p}}_j = \mathbf{p}_j + \mathbf{n}_j$ and a vector of parameters θ used to model that data, the posterior probability is

$$\pi(\theta|\tilde{\mathbf{p}}_j) = \frac{\pi(\theta)\pi(\tilde{\mathbf{p}}_j|\theta)}{\pi(\tilde{\mathbf{p}}_j)}, \quad (5)$$

where $\tilde{\mathbf{p}}_j$ is the pressure vector of size N, $\tilde{\mathbf{n}}_j$ the noise, $\pi(\tilde{\mathbf{p}}_j)$ is the evidence, $\pi(\tilde{\mathbf{p}}_j|\theta)$ the likelihood and $\pi(\theta)$ the prior. The posterior is a measure of how well the model, given these parameters, explains the measured data. The goal of the inference is to find those parameters θ that maximize the posterior distribution. From Eq. (5), maximizing the posterior is proportional to maximizing the likelihood.

In the particular case where the noise is normally distributed and independent for each receiver $\mathbf{n}_j \sim \mathcal{N}(0,\Sigma_{\mathbf{n}_j})$, the measured pressure at each receiver is also normally distributed $\tilde{\mathbf{p}}_j \sim \mathcal{N}(\mathbf{p}_j,\Sigma_{\mathbf{n}_j})$, where $\Sigma_{\mathbf{n}_j}$

is the covariance. The mean of the distribution is Eq. (1) and the variance is the background noise. The likelihood is

$$\pi(\tilde{\mathbf{p}}_j|\theta) = \prod_{j=1}^{J} \frac{e^{-\frac{1}{2}\left((\tilde{\mathbf{p}}_j - \mathbf{p}_j(\theta))^\top \Sigma_{\mathbf{n}_j}^{-1}(\tilde{\mathbf{p}}_j - \mathbf{p}_j(\theta))\right)}}{(2\pi)^{\frac{N}{2}}|\Sigma_{\mathbf{n}_j}|^{\frac{N}{2}}}. \quad (6)$$

The covariance $\Sigma_{\mathbf{n}_j}$ plays a main role in modelling the data, because it links the dependency between the different subspaces (in this case, frequencies). If frequencies are assumed independent, maximizing the likelihood simplifies to a least squares problem.

In high dimensional and complex models, however, the computation of the posterior distribution is usually intractable analytically. In this experiment the Hamiltonian Monte Carlo (HMC) technique is used to approximate the posterior distribution $\pi(\theta|\tilde{\mathbf{p}}_j)$ by drawing samples of θ in an efficient way [14]. The use of this technique makes the Bayesian inference modelling more flexible for including additional parameters.

3.3.1 Bayesian Inference of Propagation Model Parameters

Focusing on the model in Eq. (3), the parameters that are considered uncertain are the position of sources and receivers and the reflection coefficient. In addition, the transfer-functions measured in the control areas are contaminated with background noise. These noisy parameters are represented with a tilde. Figure 2 shows the inference diagram and the relationship between the uncertain parameters $\theta = (\mathbf{r}, \mathbf{s}, \sigma)$.

The error that affects each parameter is the combination of two: known and unknown uncertainties [15]. Setting proper prior distributions requires prior information about the parameters (e.g. physical constrains, known uncertainties). As an illustrative example let us look at the measurement of the loudspeaker positions. If a distance meter is used, its technical specifications will reveal its accuracy, which comes from empirical evidence. This is considered a known uncertainty. However, other factors such as errors in the manipulation of the device, may affect the measurements. These are unknown uncertainties.

To take into account both contributions, normal distributions are used in all the parameters. This allows to
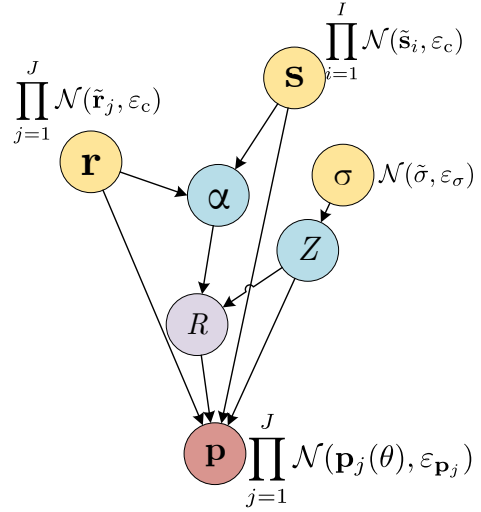

Fig. 2: Inference diagram describing the relationship between the parameters of the propagation model.

constrain the variance with the known uncertainty and be more specific than a uniform distribution, while still making it possible to sample in entire $\mathbb{R}$, thus accounting for unknown uncertainties.

The mean of source and receiver coordinates are the measured values $\tilde{\mathbf{s}}$ and $\tilde{\mathbf{r}}$. The deviation ε_c is the same for all of them, as the same measurement device and procedure is assumed. The flow resistivity is usually not measured, but taken from existing tables that group different types of grounds. If Nord2000 is used, flow resistivity's mean should be the representative value $\tilde{\sigma}$ of the selected Nordtest [16] impedance class. The standard deviation ε_σ has to be sufficiently large to ensure sampling in the entire flow resistivity range of mentioned class. The flow resistivity cannot be less than 0, therefore the normal distribution is truncated to account only for positive values. The noise in the measured pressure data is considered independent for each position as each receiver might be affected by different noise in a real scenario. For the sake of simplicity it is modelled constant over frequency.

3.4 Setup

Sound field optimization and parameter estimation is illustrated here with simulations for a simple case resembling a small, open air concert setup in which the
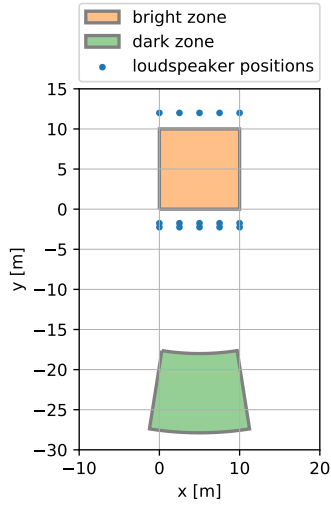
Fig. 3: Setup of bright zone, dark zone and fixed loud-speaker positions in the simulation.

radiation of sound to a sensitive area behind the concert is to be mitigated.

The setup is shown in Figure 3. The bright zone is bounded by two loudspeaker arrays with 5 and 10 loud-speakers, respectively. The target field in the bright zone is a 100 dB SPL plane wave travelling in negative y-direction. The dark zone is placed 17.5 m away from the bright zone. Both zones are sampled at 2.5 evaluation points per maximum wavelength in each direction. The frequency range of interest is from 20 to 250 Hz with a frequency resolution of 15.33 Hz. Both evaluation points and loudspeakers are positioned 1.6 m above the ground. The ground is considered compacted park area (Impedance Class E according to Nordtest) with $\sigma = 700 \, \text{kPa} \cdot \text{m/s}$. The speed of sound is $c = 343 \, \text{m/s}$ and air density $\rho = 1.2 \, \text{kg/m}^3$.

The dark zone mean square pressure is bounded to be less than 60 dB SPL, i.e. $D_0 = 20 \, \mu\text{Pa} \times 10^{60/10}$. The regularization parameter was chosen ad-hoc to $E_0 = 50 \, \text{m}^6\text{s}^{-3}$, as it leads to reasonable solutions for this problem. Too much regularization will reduce the achieved acoustic contrast between sound zones, while too little regularization will increase the sensitivity of the solution to the errors in the model parameters. Choosing the right regularization parameter is non-trivial and out of the scope of this paper (see e.g. [17]).

Table 1: Summary of relevant parameters and its chosen values in the setup.

Parameter		Value
D_0	Max. mean squared pressure in DZ	$20 \, \mu\text{Pa} \times 10^{60/10}$
E_0	Regularization parameter	$50 \, \text{m}^6\text{s}^{-3}$
SNR	Signal to Noise Ratio	30 dB
-	Coordinates Error	15 cm
σ	True Flow Resistivity	700 kPa·m/s
$\tilde{\sigma}$	Forward Flow Resistivity	500 kPa·m/s
$\varepsilon_{\mathbf{c}}$	STD Coordinates	30 cm
ε_{σ}	STD Flow Resistivity	500 kPa·m/s
$\varepsilon_{\mathbf{p}_j}$	STD Sound Pressure	$\mathcal{U}(0, \inf)$

3.4.1 Noise and Uncertainties

In order to resemble real conditions in the simulations, measurement noise and uncertainties need to be generated for the desired parameters. Measured coordinates of both sources and evaluation points, $\tilde{\mathbf{r}}$ and $\tilde{\mathbf{s}}$, are affected by 15 cm of deviation. Measured pressure $\tilde{\mathbf{p}}$ is distorted with 30 dB SNR noise for all the frequencies.

The statistical parameters used during the Bayesian inference are summarized in Table 1. The deviation of the coordinates is set to $\varepsilon_{\mathbf{c}} = 30$ cm in the prior, accounting for the known and unknown uncertainties (the known deviation of a common laser meter is less than 1 cm). The ground is considered park area, so $\tilde{\sigma}$ is set as the representative value of the Impedance Class E in Nordtest $\tilde{\sigma} = 500 \, \text{kPa} \cdot \text{m/s}$. The standard deviation $\varepsilon_{\sigma} = 500 \, \text{kPa} \cdot \text{m/s}$ to ensure sampling in the entire flow resistivity range of the Impedance Class E. The variance of the pressure $\varepsilon_{\mathbf{p}_j}$ is a uniformly distributed variable only constrained to be greater than 0.

The frequencies used during the parameter inference are the center frequencies of the third octave bands from 50 to 8000 Hz. STAN is used as the software platform to calculate the inference [18]. To compute the posterior distribution 4 HMC chains of 4000 samples were run in parallel to reach convergence. Only the second half of the samples is considered to belong to the posterior distribution and the first half is dropped as part of the warm up process of the random walk.

4 Results

4.1 Parameter Inference Model and Estimation

Figures 4 to 6 show the prior and the posterior probability density functions for the flow resistivity and the
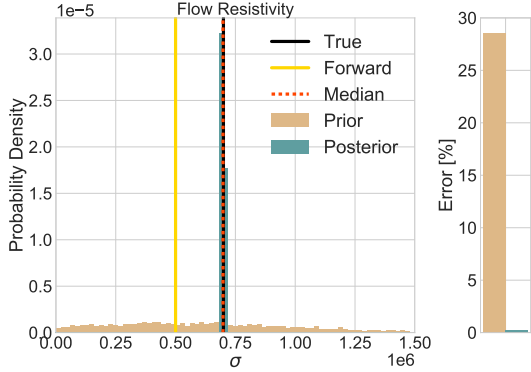
Fig. 4: Inference of flow resistivity: prior distribution $\pi(\sigma)$ vs. posterior distribution $\pi(\sigma|\tilde{\mathbf{p}}_j)$.

Fig. 5: Inference of source coordinates: prior distribution $\pi(\mathbf{s})$ vs. posterior distribution $\pi(\mathbf{s}|\tilde{\mathbf{p}}_j)$.
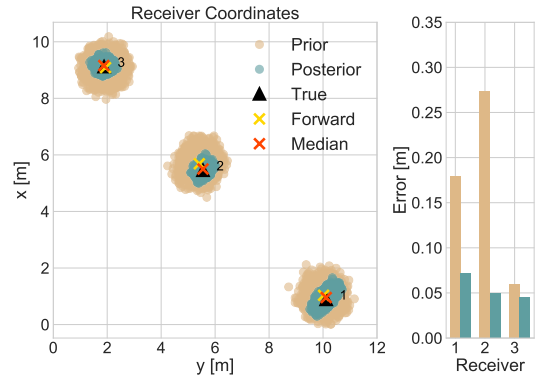
Fig. 6: Inference of receiver coordinates: prior distribution $\pi(\mathbf{r})$ vs. posterior distribution $\pi(\mathbf{r}|\tilde{\mathbf{p}}_j)$.
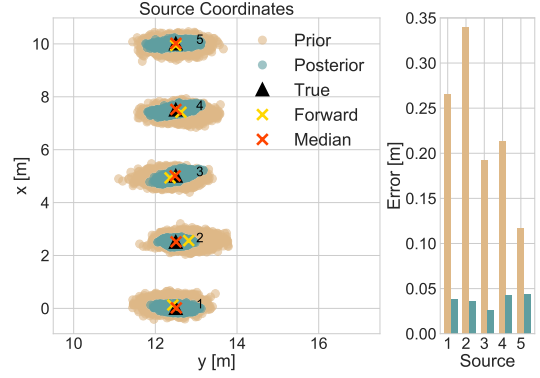
coordinates of 5 sources (the ones in the upper part of Figure 3) and 3 receivers arbitrarily picked from the bright zone, respectively. The yellow values, called forward values, are the noisy parameters. Those are the ones that may be used in a traditional forward propagation model. The black values are the correct values (no noise) named true. The median of each posterior distribution, shown in red, is chosen as the optimized parameter. The vertical bar plots at the right side of each graph represent the error from the forward and the posterior median to the true value respectively.

The posterior distribution of the flow resistivity $\pi(\sigma|\tilde{\mathbf{p}}_j)$ is much more narrower than the prior, reducing the uncertainty to a standard deviation of $\varepsilon_{\sigma|\tilde{\mathbf{p}}_j} \simeq 4000\,\mathrm{kPa \cdot m/s}$. The forward $\tilde{\sigma}$ is not considered anymore as a possible solution (out of the bounds of the posterior), while the true flow resistivity of the ground is. When comparing the optimized flow resistivity calculated as the median of the posterior with the forward guess, the error drops from $\sim 28\%$ to less than 1%.

The estimate of the sources and receivers coordinates have also been improved by the Bayesian inference. The standard deviation is $\varepsilon_{c|\tilde{\mathbf{p}}_j} \simeq 7.5$ cm, reducing to half the prior uncertainty. In addition, the error of choosing the median as point estimate is less than 5 cm for all the points except one (Receiver 1).
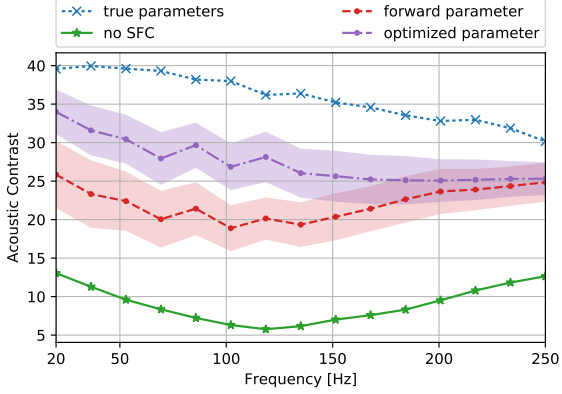
4.2 Sound Field Optimization

The acoustic contrast between dark and bright zones is defined as the mean spatial difference between SPL in

Fig. 7: Mean acoustic contrast between the bright and dark zones. The red and blue areas mark the variation of one standard deviation when using the uncertain initial and inferred model parameters, respectively.

the two zones, (e.g. [19]),

$$AC_j = 10\log_{10}\left(\frac{\frac{1}{J_{\text{BZ}}}\sum_{j\in BZ}|p_j^{(n)}|^2}{\frac{1}{J_{\text{DZ}}}\sum_{j\in DZ}|p_j^{(n)}|^2}\right). \qquad (7)$$

Figure 7 compares the acoustic contrast with and without sound field control in the cases of true parameters, forward parameters and optimized parameters. No sound field control describes the case where only the upper loudspeaker array is active with constant source strengths. That contrast is only due to the distance of the zones to the sources. Applying the sound field control system improves the acoustic contrast by 17 dB-35 dB in the ideal case of true parameters. If the forward parameters are used without inference, the improvement reduces considerably to around 10 dB, even though the uncertainty in the positions is small compared to the wavelength. Using Bayesian inference to optimize the contrast enhances the improvement again to 10 dB-21 dB. The inference improves the contrast especially in the low frequencies, where the source strengths are large (not shown) and thus where the resulting sound field is sensitive to errors.

The target plane wave and resulting sound field in the bright zone are compared in figure 8. The plane wave sound field is well reproduced when the distance between loudspeakers is much smaller than the wavelength.
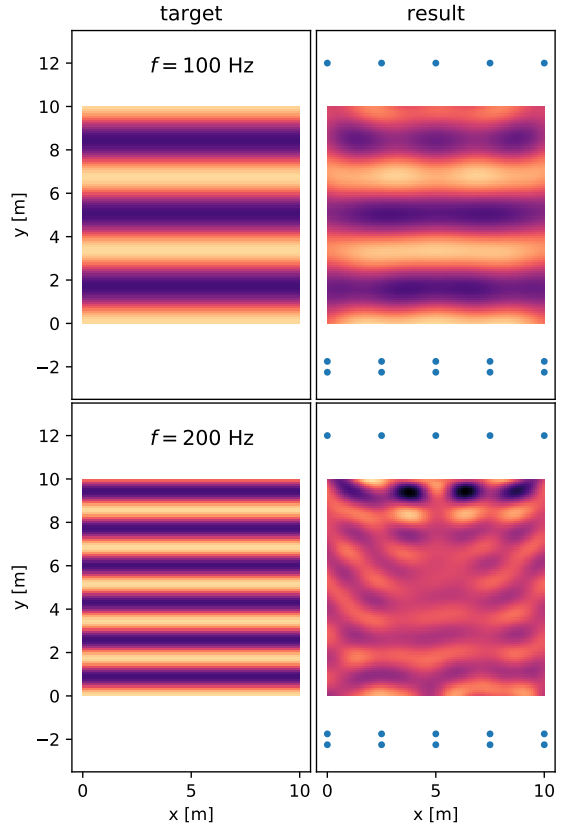
Fig. 8: Comparison of target and resulting sound pressure field in the bright zone at two frequencies. Loudspeaker positions shown as blue dots.

Figure 9 shows the SPL distribution in the vicinity of the setup. Notice how the solution creates an acoustic shadow or region of destructive interference in the dark zone and thereby reduces the SPL in that area. However, just left and right to the dark zone, the SPL increases drastically (cf. section 5.1).

5 Discussion

The addition of more data is linked to a better Bayesian inference of the parameters that depend on that new data. Adding more receivers ($J \uparrow$) means that more measured data is available to infer source coordinates and flow resistivity, calculating a posterior with less deviation. When adding more sources ($I \uparrow$) but keeping the number of receivers, the scenario starts to grow in complexity without having more data that explains the problem. Convergence in this cases is not always achieved for every run. However, when it is achieved, the inference of sigma is less uncertain, because the solution is satisfying the propagation model for more source-receiver pairs.

The addition of more measured data is linked to increasing the SNR in the pressure measurements. This effect can be compared to the averaging technique in order to reduce the background noise.

To have a closed solution of the transfer-functions, point estimates need to be calculated. The median of the posterior density functions is picked as the optimized parameters. The idea is to avoid skewed point estimates that may appear when using the mean instead.

The setup used in the simulation (figure 3) is only reducing the sound pressure level in a specific area. Using more loudspeakers will enable control over a larger area. To reduce the SPL everywhere outside the bright zone, Chang and Jacobsen [1] proposed to surround the bright zone completely with a double layer loudspeaker array at the expense of a large number of loudspeakers. This solutions becomes infeasible for large scale application.

It should also be noted that the dark zone in the setup is inside the near-field of the loudspeaker array. The far-field radiation pattern will thus not necessarily have a minimum in the negative *y*-direction and the SPL could therefore increase behind the dark zone.

So far we have only investigated the sound zoning problem in a 2D plane parallel to the ground. If there is an uneven terrain or close by buildings, both the loudspeaker arrays and sound field evaluation points need to be extended in the height dimension to account for 3D control zones.

5.1 Challenges

The results presented in this paper show how sound field optimization and parameter estimation can be applied to the noise problem of outdoor concerts. A real implementation of such a sound field control system will have to cope with a variety of additional issues, some of which we would like to highlight here.

Filter delays: the frequency domain filters obtained through the sound field optimization, especially when real transfer-function data is used, are not necessarily causal and require a modelling delay of typically half the filter length for real time implementation. This can be a problem for live-music, where the delay between the musician and the sound reinforcement system must be small. Simón Galvez et al. [20] have proposed a time-domain formulation of the sound zone method used above, which allows for the solution of causally constrained filters.

Choice of target sound field: in the simulations above, we used a plane wave as the target field in the bright zone. However, the sound field at open air venues is hardly similar to a plane wave and such a choice is a strong restriction on solutions of the optimization. Coleman et al. [21] have proposed planarity control, which introduces a controllable degree of freedom in the direction of propagation of the target plane wave at each frequency, leading to favorable contrast and perceived audio quality in comparison to pressure matching and acoustic contrast control in a sound zone setup [22]. To the knowledge of the authors, quantitative measures for the perception of low frequency audio quality have not yet been thoroughly investigated, leaving the optimal target sound field in a perceptive sense still as an open question.

Increase of sound energy: a classic result of sound power interaction of coherent sources is that in free field a control source has to be closer than half a wavelength to a noise source to be able to reduce the total emitted sound power effectively (see e.g. [23]). A separate loudspeaker array, like the lower array in figure 3, will thus not work as an active absorber, but rather create destructive interference in some area at the expense of higher sound pressure levels at other positions.

8
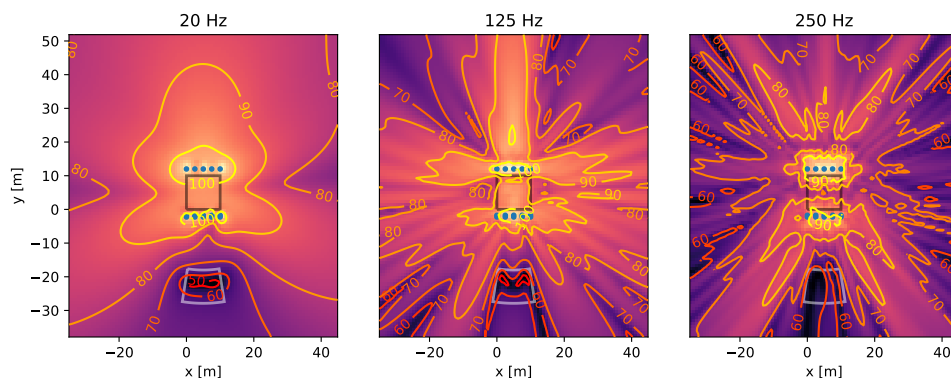
Fig. 9: SPL in dB in the vicinity of the simulated venue for the solution with true model parameters.

Care must be taken in designing the loudspeaker arrays and optimization problem, such that the reduction of noise levels in the dark zone does not lead to new noise problems in other areas.

Accuracy of propagation model: Several important phenomena are not included in the model such as temperature, wind effect, scattering, atmospheric absorption, heterogeneous ground and diffraction [24]. Many of them generate epistemic (reducible) uncertainties while others are purely aleatory provoking incoherent interference between sources [25]. The need of phase information in the transfer-functions for control purposes makes it necessary to improve the formulation of traditional outdoor sound propagation models such as Nord2000.

Wind: If multiple sources create a complex sound field through constructive and destructive interference, the resulting sound field will be sensitive to changes in the phase relationship between evaluation point and the sources. Wind effectively changes the speed of sound and will thus have a strong impact on this phase relation.

6 Summary

This paper introduces the first ideas for a sound field control system for outdoor concerts. We propose the use of a propagation model for estimation of the transfer-functions, as a their direct measurement is infeasible when controlling large areas. The uncertain parameters of the propagation model are optimized using Bayesian inference on the data obtained from a small set of transfer-function measurements. Through a simple simulation, we show that this parameter tuning can improve the acoustic contrast created by the sound field control system in comparison to using traditional propagation modelling. Finally, some additional challenges of controlling the sound outdoors in large scale are highlighted, which will be the focus of future work.

7 Acknowledgements

References

[1] Chang, J.-H. and Jacobsen, F., "Sound field control with a circular double-layer array of loudspeakers," *The Journal of the Acoustical Society of America*, 131(6), p. 4518, 2012.

[2] Chang, J.-H. and Jacobsen, F., "Experimental validation of sound field control with a circular double-layer array of loudspeakers," *The Journal of the Acoustical Society of America*, 133(4), p. 2046, 2013.

[3] Betlehem, T., Zhang, W., Poletti, M. A., and Abhayapala, T. D., "Personal Sound Zones: Delivering interface-free audio to multiple listeners," *IEEE Signal Processing Magazine*, 32(2), pp. 81–91, 2015.

[4] Kim, K., Ryu, H., and Wang, S., "Directivity Control of a Large Loudspeaker by Multi-zone Control using Small Loudspeaker Array," in *Internoise 2016*, pp. 528–535, 2016.

[5] Choi, J.-W. and Kim, Y.-H., "Generation of an acoustically bright zone with an illuminated region using multiple sources," *The Journal of the Acoustical Society of America*, 111(4), pp. 1695–1700, 2002.

[6] Sadri, M., Brunskog, J., and Younesian, D., "Application of a Bayesian algorithm for the statistical energy model updating of a railway coach." *Applied Acoustics*, 112, pp. 84–107, 2016.

[7] Cheung, S. H. and Beck, J. L., "Bayesian Model Updating Using Hybrid Monte Carlo Simulation with Application to Structural Dynamic Models with Many Uncertain Parameters," *Journal of Engineering Mechanics*, 135(4), pp. 243–255, 2009.

[8] Kung, W. T., Lee, Y. Y., and Sun, H. Y., "Sound leakage identification for an enclosed room using the probabilistic approach and model class selection index: An experiment," *Journal of Sound and Vibration*, 310(4-5), pp. 776–781, 2008.

[9] MONICA Project, http://www.monica-project.eu/, 2017, [Online; accessed 13.6.2017].

[10] Boyd, S. and Vandenberghe, L., *Convex optimization*, Press, Cambridge University, 7th edition, 2010.

[11] Jones, E., Oliphant, T., Peterson, P., et al., "SciPy: Open source scientific tools for Python," http://www.scipy.org/, 2001–, [Online; accessed 1.5.2017].

[12] Plovsing, B., "Proposal for Nordtest Method: Nord2000 - Prediction of Outdoor Sound Propagation," http://assets.madebydelta.com/docs/share/Akustik/nord2000_nordtestproposal_rev4.pdf, 2014.

[13] Miki, Y., "Acoustical properties of porous materials-Modifications of Delany-Bazley models," *J. Acoust. Soc. Jpn.(E)*, 11(1), pp. 19–24, 1990.

[14] Gelman, A., Carlin, J. B., Stern, H. S., Dunson, D. B., Vehtari, A., and Rubin, D. B., *Bayesian Data Analysis*, CRC Press, 3 edition, 2014.

[15] Chow, C. C. and Sarin, R. K., "Known, Unknown and Unknowable Uncertainties," *Theory and Decision*, 52, pp. 127–138, 2002.

[16] Nordtest Team, http://www.nordtest.info, 2014, [Online; accessed 10.6.2017].

[17] Coleman, P., Jackson, P. J., Olik, M., Olsen, M., Møller, M., and Pedersen, J. A., "The influence of regularization on anechoic performance and robustness of sound zone methods," *Proceedings of Meetings on Acoustics*, 19(1), 2013.

[18] Stan Development Team, "PyStan: the Python interface to Stan, Version 2.15.0.0." http://mc-stan.org, 2017, [Online; accessed 12.6.2017].

[19] Olsen, M. and Møller, M. B., "Sound zones: on the effect of ambient temperature variations in feed-forward systems," in *AES 142nd Convention*, 2017.

[20] Simón Galvez, M. F., Elliott, S. J., and Cheer, J., "Time Domain Optimization of Filters Used in a Loudspeaker Array for Personal Audio," *IEEE/ACM Transactions on Audio, Speech, and Language Processing*, 23(11), pp. 1869–1878, 2015.

[21] Coleman, P., Jackson, P. J. B., Olik, M., and Abildgaard Pedersen, J., "Personal audio with a planar bright zone," *The Journal of the Acoustical Society of America*, 136(4), pp. 1725–1735, 2014.

[22] Baykaner, K., Coleman, P., Mason, R., Jackson, P. J. B., Francombe, J., Olik, M., and Bech, S., "The relationship between target quality and interference in sound zones," *AES: Journal of the Audio Engineering Society*, 63(1-2), pp. 78–89, 2015.

[23] Jacobsen, F. and Juhl, P. M., *Fundamentals of General Linear Acoustics*, Wiley, 2013.

[24] Attenborough, K., "Handbook of Acoustics," chapter 4, pp. 137–155, Springer, 2nd edition, 2014.

[25] Wilson, D. K., Pettit, L. P., Ostashev, V. E., and Vecherin, S. N., "Description and quantification of uncertainty in outdoor sound propagation calculations)," *The Journal of the Acoustical Society of America*, 3(136), pp. 1013–1028, 2014.